ISSN 1063-7826, Semiconductors, 2015, Vol. 49, No. 7, pp. 939–943. © Pleiades Publishing, Ltd., 2015.
Original Russian Text © L.S. Golobokova, Yu.V. Nastaushev, F.N. Dultsev, N.V. Kryzhanovskaya, E.I. Moiseev, A.S. Kozhukhov, A.V. Latyshev, 2015, published in Fizika i Tekhnika Poluprovodnikov, 2015, Vol. 49, No. 7, pp. 961–965.

SEMICONDUCTOR STRUCTURES, LOW-DIMENSIONAL SYSTEMS, AND QUANTUM PHENOMENA

Optical and Electrical Properties of Silicon Nanopillars

L. S. Golobokova[a]*, Yu. V. Nastaushev[a], F. N. Dultsev[a], N. V. Kryzhanovskaya[b], E. I. Moiseev[b], A. S. Kozhukhov[a], and A. V. Latyshev[a]

[a] *Rzhanov Institute of Semiconductor Physics, Siberian Branch, Russian Academy of Sciences, Novosibirsk, 630090 Russia*
[b] *St. Petersburg Academic University—Nanotechnology Research and Education Center of the Russian Academy of Sciences, St. Petersburg, 194021 Russia*
**e-mail: golobokovals@isp.nsc.ru*

Submitted December 24, 2014; accepted for publication December 31, 2014

Abstract—The electrical and optical properties of silicon nanopillars (Si NPs) are studied. Electron-beam lithography and reactive ion etching are used for the formation of ordered Si-NP arrays. The Si NPs with a diameter from 60 to 340 nm and a height from 218 to 685 nm are formed. The Si NPs are coated with a $TiON_x$ layer with a thickness of 8 nm for chemical and electrical passivation of the surface. Scanning electron microscopy and atomic-force microscopy are used to characterize the obtained structures. The Si-NP arrays acquire various colors when exposed to "bright-field" illumination. The spectra of reflection from the Si-NP arrays in the wavelength range 500–1150 nm are obtained.

DOI: 10.1134/S1063782615070088

1. INTRODUCTION

The physical properties of silicon nanostructures, such as porous silicon, nanowires, and nanopillars, are much different from the properties of bulk silicon [1–3]. In recent times, such structures have attracted considerable attention. Through their use, one can increase the efficiency and improve the characteristics of various devices: photodetectors [4], solar cells [5, 6], nanosensors [7], and so on.

In this study, we investigate the optical and electrical properties of silicon nanopillars (Si NPs). The Si NPs were formed using electron-beam lithography with subsequent reactive ion etching. Electron-beam lithography (EBL) and reactive ion etching are widely used for the formation of Si NPs and also various structures of photonic crystals. Typically, in this situation, silicon structures are etched in plasma through a mask of aluminum [7] or chromium [8], which gives rise to the additional doping of silicon. As a result, new recombination centers are formed; this detrimentally affects the electronic and optical properties of structures. In this study, silicon is etched through a mask made of resist. The method of atomic-force microscopy (AFM) is used to study the morphology and electrical properties of individual Si NPs. In order to determine the conductivity of the Si NPs using an NTEGRA (NT-MDT) AFM, we measure the current–voltage (I–V) characteristics of individual Si NPs.

We demonstrate a variation in the color of the Si NPs, which is detected using an Imager Z1m microscope (Carl Zeiss, Germany) under bright-field conditions in reflected light. The intense resonance scattering of white light by individual silicon nanowires was first observed in 2010 [8, 9]. It is assumed that this effect is caused by the phenomenon of the capture of light-wave energy by a nanowire at the wavelengths of some optical resonances. A variation in the color of nanostructured silicon surface formed during the course of anisotropic two-stage plasma-chemical etching (the Bosch process) is attributed [10] to the capture of a fraction of the incident radiation by waveguide edge modes and by scattering of the remaining radiation at the surface. Ordered Si-NP arrays [11] are theoretically considered as a model of a photonic crystal; therefore, as the NP period is decreased in the array, the effect of the Bloch modes in a photonic crystal is increased. A variation in the Si-NP color is also related to the Mie resonances [12, 13]. In our study, we perform experimental investigations of the effect of the scattering of light at Si NPs and we investigate the effect of surface passivation on the NP properties. We measure the spectra of reflection from the Si NP arrays.

2. EXPERIMENTAL

As substrates, we used single-crystal n-type Si (100) wafers. The general scheme of technological cycles of Si-NP formation using the EBL is shown in Fig. 1. Electron lithography was performed using Pioneer and Raith 150 (Raith GmbH) setups. As a negative electron resist, we used ma-N2403 (phenoaldeghid-polymer). After carrying out preliminary peroxide–ammonia treatment of the silicon surface, the resist was deposited by centrifugal separation with a rate of 3000 min^{-1} for 90 s (the centrifuge was a Spin 150 Wafer spinner). The resist's thickness was 300 nm.

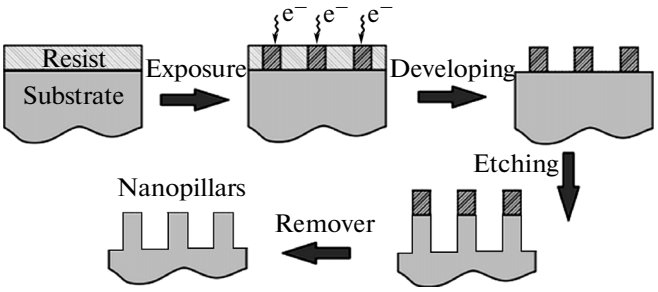

Fig. 1. Schematic representation of the formation of Si NPs.

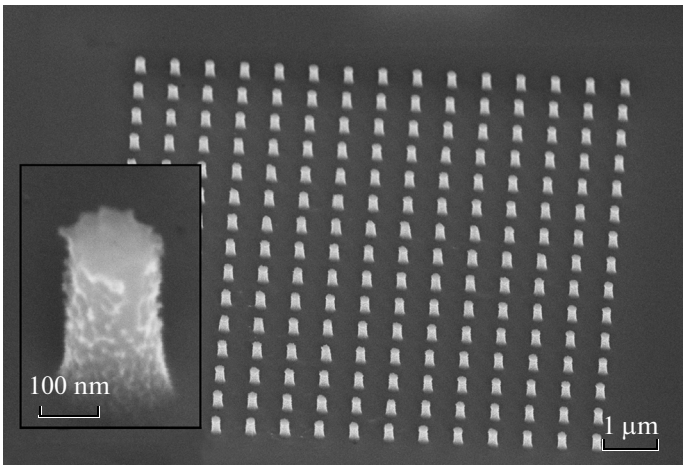

Fig. 2. SEM image of a Si-NP array and an enlarged image of an individual NP after boiling in HNO_3. The scale marks of 1 μm and 100 nm (on the inset).

Exposure of the resist to electrons was conducted at an accelerating voltage of 20 or 30 kV at different beam currents (from 10 to 200 pA). To form a mask in the resist in the form of arrays of pillars of various diameters, the electron dose per point was varied in the range 0.01–0.1 pC. The pillar diameter was changed by varying the radiation dose. Development of the image in the resist was attained in an ma D525 developer for 150 s. The Si NPs were formed under the reactive ion etching of silicon through a mask composed of a negative electron resist. Etching was performed under various conditions using Plasmalab System 100 and Matrix setups. The use of plasma etching made it possible to ensure a high anisotropicity, high selectivity, and the required aspect relation of structures with Si NPs. For etching to a depth of 300 nm, we used mixtures of SF_6/N_2 and CF_2Cl_2/Ar gases. For deep etching of silicon (to a depth of 600 nm and larger), we used anisotropic plasma etching using a mixture of SF_6/C_4F_8 in a two-stage cyclic mode (the Bosch process) [14]. The power of the high-frequency discharge was varied from 150 to 250 W. The power of the source of the inductively coupled plasma (ICP) was varied from 100 to 350 W. The duration of etching was varied from 10 to 120 s. During the stage of passivation, a fluorine–carbon polymer film was deposited in the C_4F_8 plasma. In order to remove the remainder of the mask of the negative resist ma-N2403 we used ma-rem 404 and short etching in oxygen plasma. The Bosch process makes it possible to attain a large depth of etching without the need for an increase in the thickness of the resist mask.

Using electron-beam lithography and reactive ion etching, we achieved precise control over the location, diameter, and height of NPs. Prior to performing the electrical and optical measurements, we annealed the studied samples with Si NPs with the use of microwave radiation in a Matrix setup for the plasma-chemical etching of semiconductors. The power of the HF discharge (with a frequency of 13.56 MHz) was 100 W. The duration of microwave annealing was 1 min. In order to attain chemical and electrical passivation of the surface, the Si NPs were coated with an insulating $TiON_x$ nanolayer formed during the course of plasma-chemical nitridation of the titanium nanolayer [15]. Passivation of the surface was performed in order to decrease the density of surface states and reduce the surface recombination of charge carriers. We also performed passivation by the method of boiling in concentrated nitric acid, as a result of which silicon oxide was formed. Oxidation in nitric acid was required for samples formed by the Bosch method in order to remove the polymer which remained on the walls of the Si NPs; in this case, insignificant heating of the NP walls was observed and roughness of the edge increased (Fig. 2).

In order to measure the conductance of the Si NPs, we used an atomic-force microscope with a conducting probe. The silicon probe was coated with a gold film with the aim of facilitating electrical contact with the NP top. Bias voltage (from −10 V to +10 V) was applied to the silicon substrate.

The reflection spectra were measured from separate microarrays of Si NPs. The light from a halogen lamp (100 W) was passed through a lens (Olympus LMPlan IR 100X, NA = 0.8) and was then directed to the Si NP array. The same lens was used to collect the signal reflected from the sample. The signal was detected using an FHR1000 monochromator and a single-channel cooled silicon photodetector under conditions of locked-in detection (locked-in detector Stanford Research SR830). The spectral resolution was ~0.08 nm.

3. RESULTS AND DISCUSSION

After etching and passivation, we performed microwave annealing of the Si NPs to activate the conductance. Passivation of the surface with a $TiON_x$ layer considerably improves the stability of the measured I–V characteristics. Oxidation in nitric acid is insufficient for passivation of the surface; the measured I–V

characteristics featured considerable instability. The I–V characteristics of individual Si NPs shown in Fig. 3 were measured for a Si NP of the same diameter located along the given curve (Fig. 4).

The I–V characteristics shown in Fig. 3 are typical of the Schottky silicon–gold barrier. The silicon–probe contact is not ideal due to the relief of the upper part of the Si NP and to the presence of an oxide layer. The differential conductance calculated from the slope of the I–V characteristic curve at large values of electric current increased linearly with an increase in the NP diameter.

In the case of illumination by the "bright-field" method, the individual Si NP featured a specific color in reflected light (Fig. 5). Each Si NP demonstrated some characteristic color, without any reference to neighboring Si NPs. A pronounced dependence of color on the NP diameter is observed. The color of the Si NPs did not change as a result of microwave annealing. After passivation of the surface, the color of the Si NPs remained the same, while the color's intensity decreased.

The observed optical effects can be explained in the context of the Mie theory [12] when light propagating in free space interacts with a Si NP, which represents a resonator with a size smaller than the wavelength, with the result that the Si NP encourages resonances in the visible region of the spectrum.

We measured the reflection spectra in the wavelength range 500–1150 nm. The spectra featured a characteristic minimum; the position of the reflection minimum changed with a variation in the Si NP diameter. A shift to the spectrum region with longer wavelengths was observed as the Si NP diameter was increased (Fig. 6). Figure 6 also shows the reflection spectrum for a silicon surface without Si NPs; the surface was structured as a result of plasma-induced etching. The spectrum does not represent any specific features; however, due to the effect of scattering, the reflection coefficient for this surface is much lower than that in the case of the typical value of the reflection coefficient for the silicon surface.

In Fig. 7, we show the reflection spectrum for NP arrays with a period of 800 nm. It can be seen from Fig. 7 that, as the NP diameter is increased, two minima are shifted; in addition, the depth of the minimum in the reflection spectrum increases. The reflection coefficient at the minimum reaches 5%. A shift of the position of the minima to longer wavelengths as the Si-NP period increases in NP arrays of the same diameter is observed. For individual arrays at a period of 400 nm, a third minimum was observed at wavelengths larger than 1 μm; we relate this minimum directly to the etched silicon surface.

The dependence of the position of the reflection minimum on the NP diameter (see Fig. 8) observed by us differs from the theoretical dependence calculated

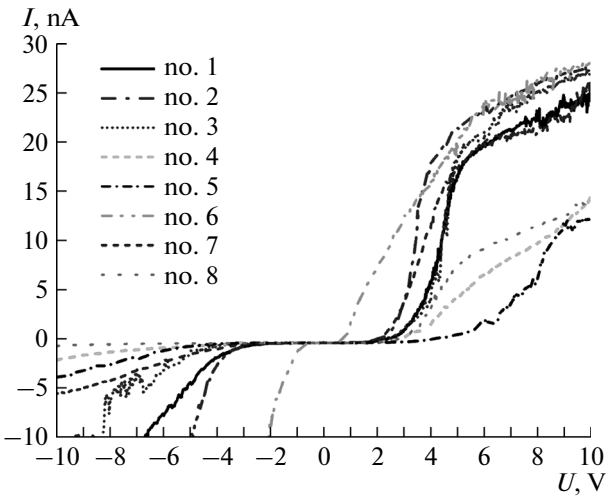

Fig. 3. I–V characteristics of Si NPs (nos. 1–8).

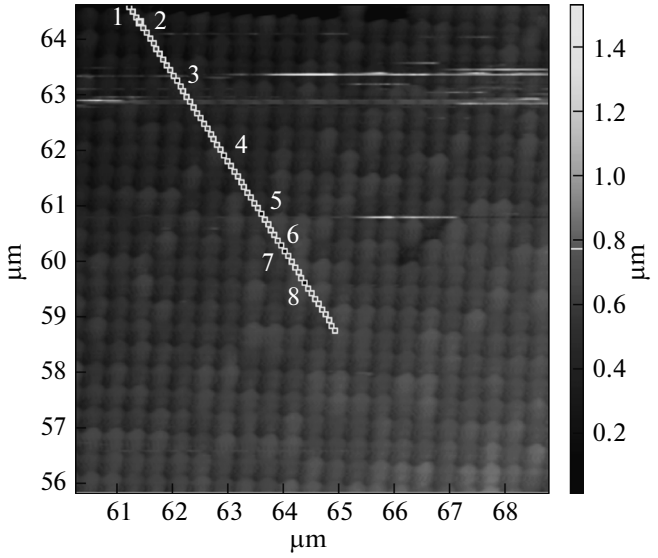

Fig. 4. AFM image of a part of a Si-NP array (the period is 0.4 μm and the height is 0.6 μm).

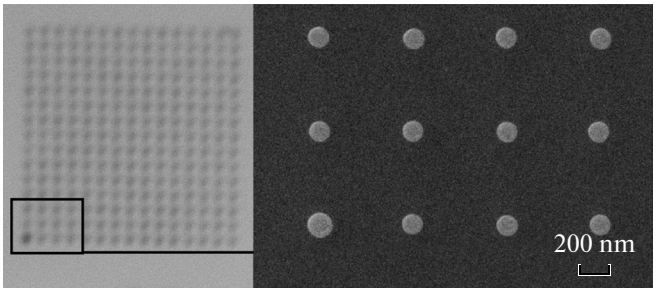

Fig. 5. Optical and SEM images (view from above) of Si NPs. The scale mark is 200 nm.

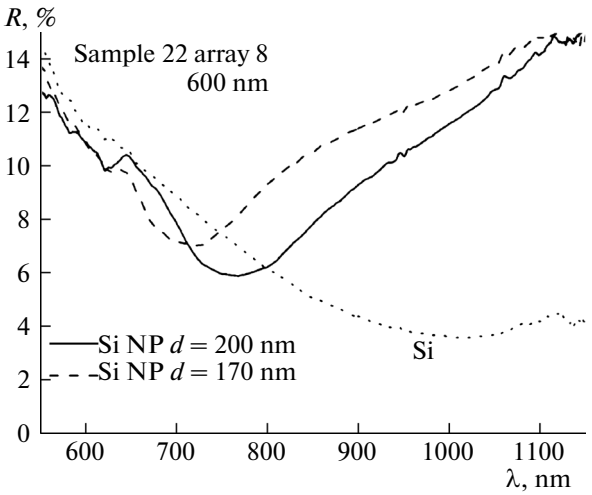

Fig. 6. Spectra of reflection from arrays of Si NPs with diameters of 200 and 170 nm; the period is 600 nm; dots show the spectrum of reflection from the surface of etched silicon, as measured away from the Si-NP array.

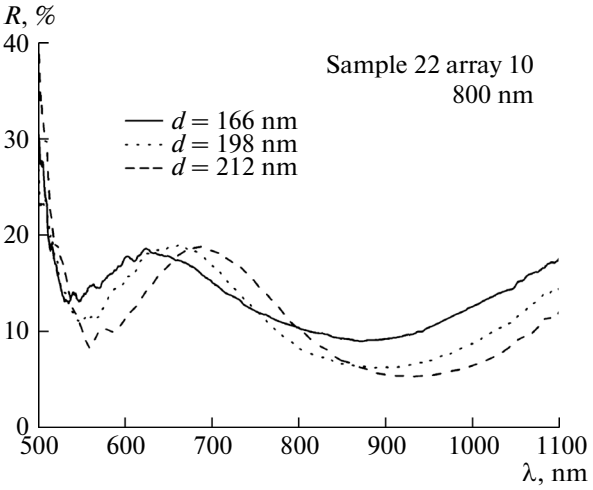

Fig. 7. Reflection spectra for Si-NP arrays with a period of 800 nm and Si-NP diameters of 166, 198, and 212 nm. The Si-NP height is 445 nm.

from the condition of observation of Mie resonance suggested in [12],

$$nkd = 2K, \quad (1)$$

where n is the refractive index, k is the wave vector, d is the diameter of a Si NP, $K \sim 2.6$ (for mode 1), and $K \sim 5.6$ (for mode 2).

This inconsistency can indicate either that formula (1) is of limited use or that, in derivation of this formula, some important factors were disregarded; these factors can affect the occurrence of resonances (roughness of the surface, curvature, and so on).

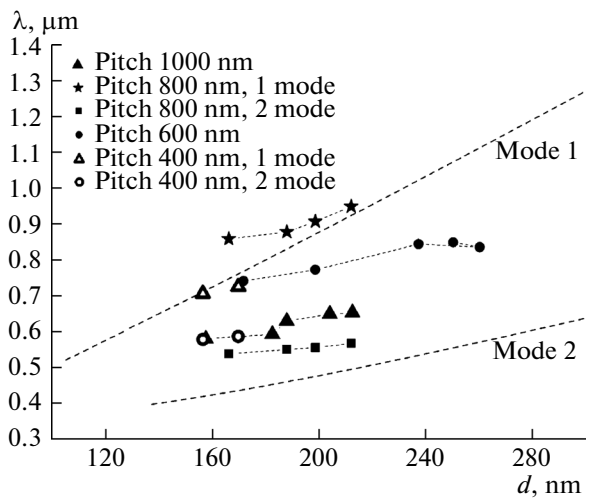

Fig. 8. Dependence of the resonance wavelength (for mode 1 and mode 2) on the Si-NP diameter. Dashed lines indicate the modes of the Mie resonance [12].

A decrease in the coefficient of the reflection of light from structures with Si NPs is related to a considerable increase in the area of the surface with Si NP arrays in comparison with a flat surface. It is important that the profile of the refractive index is modulated by an ordered array of NPs (medium–pillar–medium) while scattering occurs at an individual nanopillar.

4. CONCLUSIONS

We studied the optical and electrical properties of silicon nanopillars. In order to form arrays of nanopillars, we used electron-beam lithography and reactive ion etching through a mask of resist.

The silicon nanopillars were chemically and electrically passivated by depositing a layer of titanium oxinitride. The current–voltage characteristics were measured for individual nanopillars using the probe of an atomic-force microscope; it was found that passivation of the surface using titanium oxinitride improves the electrical properties of the nanopillars.

The effect of the pronounced resonance scattering of light (variation in the color of individual silicon nanopillars) was observed. A single minimum or several minima are observed in the measured reflection spectra; we relate these minima with the Mie resonances. One can form new media with given optical and electrical characteristics on the basis of silicon nanopillars.

ACKNOWLEDGMENTS

This study was supported in part by the Russian Foundation for Basic Research (project no. 13-02-01216).

REFERENCES

1. K. A. Gonchar, L. A. Osminkina, R. A. Galkin, M. B. Gongalsky, V. S. Marshov, V. Y. Timoshenko, M. N. Kulmas, V. V. Solovyev, A. A. Kudryavtsev, and V. A. Sivakov, J. Nanoelectron. Optoelectron. **7**, 602 (2012).
2. G. Jia, T. Arguirov, M. Kittler, Z. Su, D. Yang, and J. Sha, Semiconductors **41**, 391 (2007).
3. S. M. Wells, I. A. Merkulov, I. I. Kravchenko, N. V. Lavrik, and M. J. Sepaniak, ACS Nano **6**, 2948 (2012).
4. B. Wang and P. W. Leo, Opt. Lett. **37**, 3756 (2012).
5. Xiaocheng Li, Junshuai Li, Ting Chen, Beng Kang Tang, Jianxiong Wang, and Hongyu Yu, Nanoscale Res. Lett. **5**, 1721 (2010).
6. S. Dominguez, I. Cornago, O. Garcia, M. Ezquer, M. J. Rodriguez, A. R. Lagunas, J. Perez-Conde, and J. Bravo, Photon. Nanostruct.: Fundamentals Appl. **11**, 29 (2013).
7. M. Khorasaninejad, N. Abedzadeh, J. Walia, S. Patchett, and S. S. Saini, Nano Lett. **12**, 4228 (2012).
8. L. Cao, P. Fan, E. S. Barnard, A. M. Brown, and M. L. Brongersma, Nano Lett. **10**, 2649 (2010).
9. Seo Kwanyong, Munib Wober, Paul Steinvurzel, Ethan Schonbrun, Yaping Dan, Tal Ellenbogen, and K. B. Crozier, Nano Lett. **11**, 1851 (2011).
10. A. A. Zalutskaya and A. V. Prokaznikov, Nano-Mikrosist. Tekh. **9**, 11 (2013).
11. K. T. Fountaine, W. S. Whitney, and H. A. Atwater, J. Appl. Phys. **116**, 153106 (2014).
12. F. J. Bezares, J. P. Long, O. J. Glembocki, Junpeng Guo, R. W. Rendell, R. Kasica, L. Shirey, J. C. Owrutsky, and J. D. Caldwell, Opt. Express **21**, 27588 (2013).
13. A. B. Evlyukhin, R. L. Eriksen, Wei Cheng, J. Beermann, C. Reinhardt, A. Petrov, S. Prorok, M. Eich, B. N. Chichkov, and S. I. Bozhevolnyi, Sci. Rep. **4**, 4126 (2014).
14. Y. Q. Fu, A. Colli, A. Fasoli, J. K. Luo, A. J. Flewitt, A. C. Ferrari, and W. I. Milne, J. Vac. Sci. Technol. B **27**, 1520 (2009).
15. F. N. Dultsev, S. N. Svitasheva, Yu. V. Nastaushev, and A. L. Aseev, Thin Solid Films **519**, 6344 (2011).

Translated by A. Spitsyn